ISSN 1674-1056
http://cpb.iphy.ac.cn
http://iopscience.iop.org/cpb
中国物理 B
Chinese Physics
中国物理
Chinese Physics B

Sterilization of mycete attached on the unearthed silk fabrics by an atmospheric pressure plasma jet

Rui Zhang(张锐), Jin-song Yu(於劲松), Jun Huang(黄骏), Guang-liang Chen(陈光良), Xin Liu(刘欣), Wei Chen(陈维), Xing-quan Wang(王兴权), Chao-rong Li(李超荣)
Citation: Chin. Phys. B . 2018, 27(5): 055207. **doi:** 10.1088/1674-1056/27/5/055207

Journal homepage: http://cpb.iphy.ac.cn; http://iopscience.iop.org/cpb

What follows is a list of articles you may be interested in

Numerical study on the gas heating mechanism in pulse-modulated radio-frequency glow discharge

Qi Wang(王奇), Xiao-Li Yu(于晓丽), De-Zhen Wang(王德真)
Chin. Phys. B . 2017, 26(3): 035201. **doi:** 10.1088/1674-1056/26/3/035201

Numerical study of the effect of water content on OH production in a pulsed-dc atmospheric pressure helium-air plasma jet

Mu-Yang Qian(钱沐杨), Cong-Ying Yang(杨从影), Zhen-dong Wang(王震东), Xiao-Chang Chen(陈小昌), San-Qiu Liu(刘三秋), De-Zhen Wang(王德真)
Chin. Phys. B . 2016, 25(1): 015202. **doi:** 10.1088/1674-1056/25/1/015202

A computational modeling study on the helium atmospheric pressure plasma needle discharge

Qian Mu-Yang, Yang Cong-Ying, Liu San-Qiu, Wang Zhen-Dong, Lv Yan, Wang De-Zhen
Chin. Phys. B . 2015, 24(12): 125202. **doi:** 10.1088/1674-1056/24/12/125202

A two-dimensional model of He/O_2 atmospheric pressure plasma needle discharge

Qian Mu-Yang, Yang Cong-Ying, Chen Xiao-Chang, Liu San-Qiu, Yan Wen, Liu Fu-Cheng, Wang De-Zhen
Chin. Phys. B . 2015, 24(12): 125203. **doi:** 10.1088/1674-1056/24/12/125203

Two-dimensional numerical study of an atmospheric pressurehelium plasma jet with dual-power electrode

Yan Wen, Liu Fu-Cheng, Sang Chao-Feng, Wang De-Zhen
Chin. Phys. B . 2015, 24(6): 065203. **doi:** 10.1088/1674-1056/24/6/065203

Sterilization of mycete attached on the unearthed silk fabrics by an atmospheric pressure plasma jet*

Rui Zhang(张锐)[1,†], Jin-song Yu(於劲松)[2,†], Jun Huang(黄骏)[3,§], Guang-liang Chen(陈光良)[1,4,‡], Xin Liu(刘欣)[4], Wei Chen(陈维)[3], Xing-quan Wang(王兴权)[3], and Chao-rong Li(李超荣)[1]

[1] *Key Laboratory of Advanced Textile Materials and Manufacturing Technology and Engineering Research Center for Eco-Dyeing & Finishing of Textiles, Ministry of Education, Zhejiang Sci-Tech University, Hangzhou* 310018, *China*

[2] *Department of Chemistry and Chemical Engineering, University of New Haven,* 300 *Boston Post Road, West Haven, Connecticut* 06516, *USA*

[3] *College of Physics and Electronic Information, Gannan Normal University, Ganzhou* 341000, *China*

[4] *State Key Laboratory for Hubei New Textile Materials and Advanced Processing Technology, Wuhan Textile University, Wuhan* 430200, *China*

(Received 24 January 2018; revised manuscript received 6 March 2018; published online 26 April 2018)

The sterilization of the simulated unearthed silk fabrics using an atmospheric pressure plasma jet (APPJ) system employing Ar/O_2 or He/O_2 plasma to inactivate the mycete attached on the silk fabrics is reported. The effects of the APPJ characteristics (particularly the gas type and discharge power) on the fabric strength, physical-chemical structures, and sterilizing efficiency were investigated. Experimental results showed that the Ar/O_2 APPJ plasma can inactivate the mycete completely within 4.0 min under a discharge power of 50.0 W. Such an APPJ treatment had negligible impact on the mechanical strength of the fabric and the surface chemical characteristics. Moreover, the Ar ions, O and OH radicals were shown to play important roles on the sterilization of the mycete attached on the unearthed silk fabrics.

Keywords: unearthed silk fabric, mycete sterilization, atmospheric pressure plasma jet (APPJ), sterilization mechanism

PACS: 52.75.–d, 52.77.–j, 52.80.Hc **DOI:** 10.1088/1674-1056/27/5/055207

1. Introduction

Unearthed Chinese silk fabrics, especially cultural silk relics, carry precious cultural heritage and are essential to the study of traditional cultures, particularly the ancient aesthetic features.[1–3] Exploring the preserved relic pieces made of the unearthed silk fabrics can facilitate the understanding of our history, the appreciation of the creative power of human beings, and the revealing of the development of human society,[4–6] all of which promote the development of contemporary and future society. However, mycete cultured on these unearthed silk fabrics are known to significantly shorten the life-spans of such fabrics, which have endured a harsh environment under the ground for a long period of time. Therefore, it is of practical importance to establish protocols for sterilizing mycete while preserving the quality of the unearthed silk fabrics. The conventional methods used for sterilizing the unearthed silk fabrics are typically based on either thermal or chemical treatment, or exposure to ionizing radiation.[7] However, these conventional processes easily cause thermal damage or chemical corrosion to the sterilized pieces. Moreover, the chemical reagents are not environmentally friendly and very effective when fungus contamination is concerned.[8] Therefore, a more effective sterilization protocol for the treatment of the unearthed silk fabrics is worthwhile exploring.

Recently, the development of the plasma based sterilization technology has made tremendous progress and it has been widely used in different industries, such as medical, biological, food-processing, and agricultural applications.[9–14] For example, Natthaporn Khamsen *et al.* designed a system to produce atmospheric hybrid cold-discharge plasma (HCP) for inactivating microorganisms that commonly attach to the rice seed husk, and the cold HCP completely inactivated the pathogenic fungi and other microorganisms, enhancing the germination percentage and seedling quality.[15] Sakai *et al.* generated oxygen plasma using a narrow gap radio-frequency (RF) discharge to sterilize dental instruments.[16] The atmospheric pressure plasma jet (APPJ), which has the characteristics of high sterilization efficiency, short treatment time, no pollution, no residue, and no damage to the materials,[17,18] may be an ideal candidate for the sterilization/inactivation of mycete.

The sterilization performance of the APPJ treatment depends heavily on the active species (e.g., highly energized atoms, charged particles, electric fields, and UV

*Project supported by the National Natural Science Foundation of China (Grant Nos. 11665005, 11505032, 11547139, 51672249, and 11565003), the Zhejiang Natural Science Foundation of China (Grant No. LY16A050002), the Natural Science Foundation of Jiangxi Province, China (Grant Nos. 20161BAB211026, 20171ACB21049, and 20171BAB211012), the Science and Technology Project of Jiangxi Provincial Department of Education, China (Grant No. GJJ150981), the Program for Innovative Research Team of Zhejiang Sci-Tech University, China, and the Opening Foundation of Insititue of Textile Technology, Wuhan Texitle Universitiy, China (Grant No. GCZX201702).

†These authors contributed equally to this work.

‡Corresponding author. E-mail: glchen@zstu.edu.cn

§Corresponding author. E-mail: junhuang66@163.com

© 2018 Chinese Physical Society and IOP Publishing Ltd

radiation)[19–21] that it generates and such active species are impacted strongly by the electrode configuration, the gas flow rate, and the applied voltage.[22–24] When helium/argon (He/Ar) mixed with oxygen act as the reactive gases in the APPJ system, the active radicals are generated by bombarding with energetic electrons, which has also been identified as an important factor to determine the bacteria sterilization outcomes.[25,26]

While various APPJ systems have been reported for many different sterilization applications, to the best knowledge of the authors of this paper, no such report on the sterilization treatment of the unearthed silk fabrics has been published. Herein, an Ar/ He–O_2 APPJ system was employed to sterilize the mycete cultured on the simulated unearthed silk fabrics to study the feasibility for treating the authentic unearthed silk fabrics. The effects of the APPJ treatment time, the discharge power, and the gas type of the APPJ system on the inactivation of mycete attached to the simulated unearthed silk fabrics were investigated. The experimental data obtained in this work was used to determine the optimized sterilization parameters and the protocol employing the Ar/O_2 APPJ system was shown to be a promising candidate for the heritage protection of the authentic unearthed silk fabrics.

2. Methods

2.1. Attaching mycete on the silk fabric

In order to determine the inactivation efficiency of the unearthed silk fabrics by the APPJ system, the standard mycete strain of the Aspergillus Niger (AN) was cultured on the silk fabrics. Firstly, the AN colony was scraped with an inoculation ring and transferred into the potato dextrose agar (PDA) slant medium. Then, the inoculated slant medium was placed in the incubator, and incubated at 37 °C for 60 h to pre-activate the mycete species. After that, a ring of the pre-activated mycete species was introduced into the liquid medium (pH = 7.2–7.4) extracted from beef, and incubated at 37 °C for 60 h in the shaking incubator for fabricating the mycete suspension. All of the above operations were performed under aseptic conditions. The silk fabric pieces (1 cm×1 cm) were washed with ethanol (98.0%) in an ultrasonic cleaning machine, and sterilized by an autoclave. The inactivated silk fabric samples were soaked in the mycete suspension and are considered as the simulated unearthed silk fabric samples.

2.2. APPJ system for Aspergillus Niger sterilization

The APPJ system used for the AN sterilization is similar to that reported in our previous work.[27] Briefly, the APPJ apparatus employing one liquid electrode was specially constructed for this work and is illustrated in Fig. 1(a). The copper tube centered in the quartz tube and the potassium chloride (KCl) solution contained in the outside quartz tube acted as the inner and outer electrodes, respectively. The use of the KCl solution not only can efficiently cool the dielectric layer (quartz tube), but also reduces the total power consumption of the system. Both electrodes were connected to an ac power with a maximum peak voltage of 30.0 kV and an adjustable frequency from 8.00 kHz to 30.0 kHz. The simulated unearthed silk fabrics steeped with the mycete suspension were placed on the sample stage, and the distance between the sample stage and the APPJ outlet was set to be 1.0 cm. The interaction between the active species generated in the APPJ system and the mycete attached on the silk fabrics is illustrated in Fig. 1(b). The identification of the various reaction species in the plasma jet was carried out by OES over a wavelength range of 200–800 nm. The system was equipped with a UV–visible optical emission spectrophotometer (Andor, SR-500i-A, USA) which had three grating monochromator systems with a resolution in the 0.14–0.4 nm range. The monochromator collected light using an optical fiber. In this study, to obtain a strong and clear emission signal, a lens was used to focus the light from the APPJ on the tip of the optical fiber. The details of the treating parameters are summarized in Table 1, and the work mentioned above was performed in an aseptic environment to prevent cross contamination of the mycete.

Table 1. The operational parameters of the APPJ system used for the sterilization of the cultured AN on the simulated unearthed silk fabrics.

Influencing factor	Sample	Input power/W	Treatment time/min	He flow rate/$m^3 \cdot h^{-1}$	Ar flow rate/$m^3 \cdot h^{-1}$	O_2 flow rate/$m^3 \cdot h^{-1}$
Time	a_1/b_1	50	1	0	0.6/0.5	0/0.1
	a_2/b_2	50	2	0	0.6/0.5	0/0.1
	a_3/b_3	50	3	0	0.6/0.5	0/0.1
	a_4/b_4	50	4	0	0.6/0.5	0/0.1
	a_5/b_5	50	5	0	0.6/0.5	0/0.1
Power	c_1	30	2	0	0.6	0
	c_2	40	2	0	0.6	0
	c_3	50	2	0	0.6	0
	c_4	60	2	0	0.6	0
Gas type	d_1	50	2	0.6	0	0
	d_2	50	2	0	0.6	0
	d_3	50	2	0.5	0	0.1
	d_4	50	2	0	0.5	0.1

2.3. Plasma sterilization process

The mycete sterilization efficiency of the APPJ system was evaluated using the plate count method with a digital microscope. The samples treated by the APPJ system were soaked and diluted from 10^{-1} to 10^{-6} by the physiological saline. Then, 50.0 μL of the diluted solution was distributed on the nutrient agar medium by the pour plate method, and the fabricated samples were placed in the incubator at 37 °C for 24 h. Finally, the mycete colonies cultured on the plates were calculated. In order to reduce the experimental error, the process presented above was repeated 3 times. Additionally, the morphology of the AN spores was examined using a series digital microscope (Keyence VHX-5000, Japan) with a magnification of 500× and 1000× respectively.

2.4. Sample characterization

The morphology of the silk fabrics was characterized by a field-emission scanning electron microscope (FESEM JSM-6700F, JEOL, Japan) at an acceleration voltage of 3.0 kV. X-ray photoelectron spectra of the samples were recorded using an x-ray photoelectron spectrometer (Kratos Aixs Ultra DLD, USA) with an aluminum (mono) $K\alpha$ source (1486.6 eV). The tensile strength property of the samples was measured with an electronic universal testing machine (WDW-100 KN) controlled by a microcomputer. The Fourier transform infrared spectroscopy (FTIR) spectrometer (Nicolet 5700, Bruker, Germany) was operated in an attenuated total reflectance (ATR) mode to analyze the functional groups of the silk fabrics.

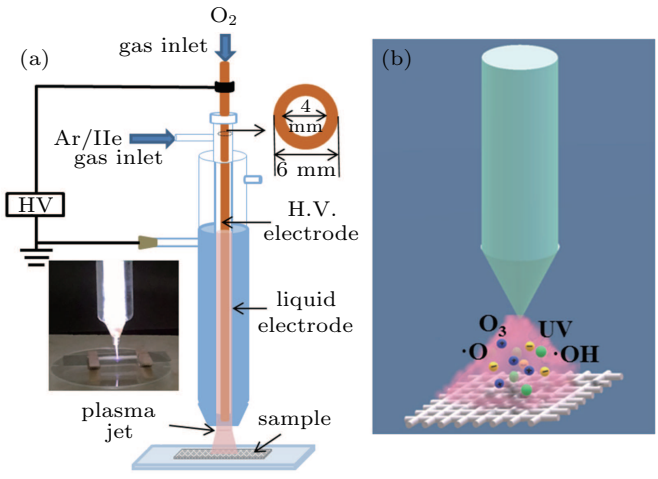


Fig. 1. (color online) Schematic illustration of (a) the plasma jet and (b) the sterilization process of APPJ.

3. Results and discussion

Figure 2 shows the optical emission spectra from 200 nm to 800 nm of Ar and He plasmas. The Ar lines mainly dominated the region of 700–800 nm and the peaks at 548 nm and 620 nm were also detected (Fig. 2(a)), and the He lines at 550 nm, 616 nm, 667 nm, and 706 nm were detected (Fig. 2(b)). Both optical emission spectra revealed the presence of excited species in the plasma jets, such as N_2, OH, H, and N_2^+. The excited O_2^+ observed at 427 nm and O emission resulting from the 3^5S–3^5P transition at 740 nm were also observed in the OES. It is well known that some of these species (e.g., O and OH) are very active in such a way that they play a very important role in sterilization of mycete. This may be due to the fact that a significant fraction of the plasma electrons used to produce O-containing species from the O_2 molecules are present in the plasma-forming gas.[28] The probable formation paths of O_2^+ in He plasma include both direct electron-impact ionization ($e^- + O_2 \rightarrow 2e^- + O_2^+$) and Penning ionization ($He(2^1S) + He(2^3S) \rightarrow He + O_2^+ + e^-$).[29,30] Since N_2 represents 70% of the ambient air, its emission is likely to be significant with respect to the intensity of O and OH emission. The presence of N_2 (265 nm, 315 nm, 337 nm, 357 nm, and 380 nm) and (378 nm and 470 nm) lines in Fig. 2 clearly revealed the presence of ambient air in the plasma, which was also reported by other researchers.[31–34] However, comparing Fig. 2(a) with Fig. 2(b), it can be found that the intensity of these species in Ar and He is obviously different, and the peak intensities of some functional species in Ar are higher than those occurred in He APPJ, which may be more effective on the mycete sterilization.

Figure 3 shows the photographs of the AN funguses attached on the silk fabrics treated different times by Ar or Ar/O_2 APPJ. As shown in Fig. 3(a_0), the number of AN colonies cultured in the PDA medium was about 110, indicating a CFU quantity of AN about 2.2×10^5 on the original untreated silk fabric. When the samples were treated by the Ar APPJ for 1 min, 2 min, 3 min, 4 min, and 5 min (Figs. 3(a_1)–3(a_5)) respectively, the AN number decreased noticeably as the plasma treatment time increased. The AN sterilization percentage could reach 99.0% if a treatment time of 5 min was used with an Ar APPJ plasma. However, the CFU number of AN on the silk fabric was still about 2×10^3, which exceeded the maximum limit when protecting the unearthed silk fabrics was concerned. Figures 3(b_0)–3(b_5) show the effect of treatment time on the AN sterilization when the Ar/O_2 APPJ was used, and the AN quantities decreased sharply as the plasma treatment time increased. Under the same discharge power as the Ar plasma, the AN attached on the untreated silk fabric (CFU: 1.36×10^5) were completely inactivated when the silk fabric was treated by the Ar/O_2 APPJ for 4.0 min (Fig. 3(b_4)), indicating that when the sterilization of mycete on the silk fabrics is concerned, the Ar/O_2 plasma will be more effective than the Ar plasma.

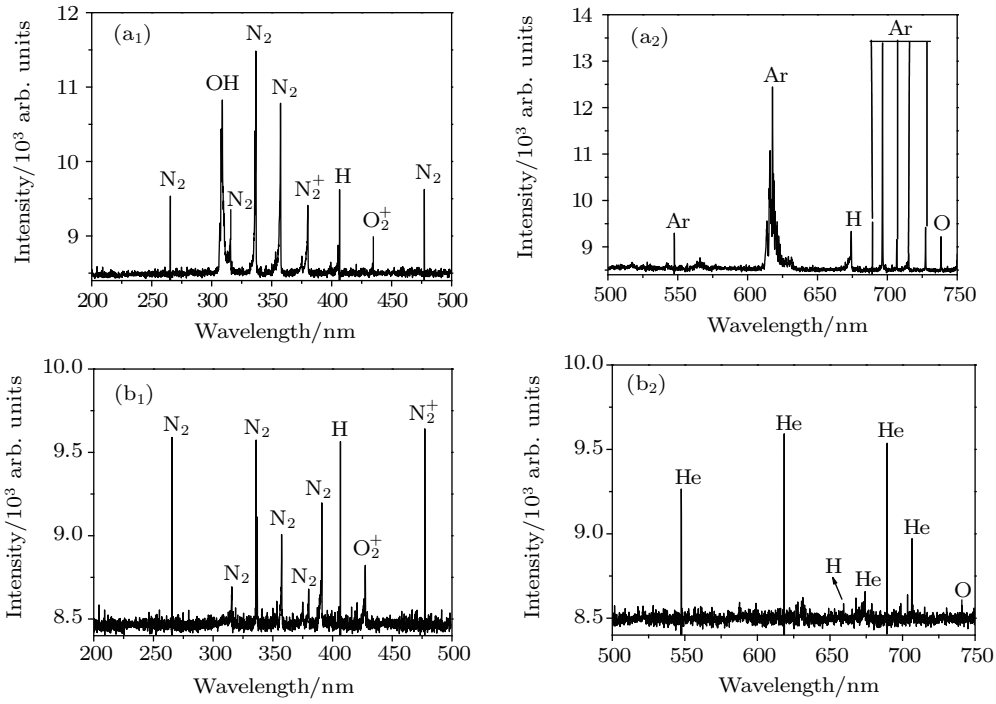


Fig. 2. Optical emission spectra of the APPJ with the silk fabrics, an Ar or He flow rate of 0.5 $m^3 \cdot h^{-1}$, an O_2 flow rate of 0.1 $m^3 \cdot h^{-1}$, and an input power of 50 W: (a) Ar, (b) He.

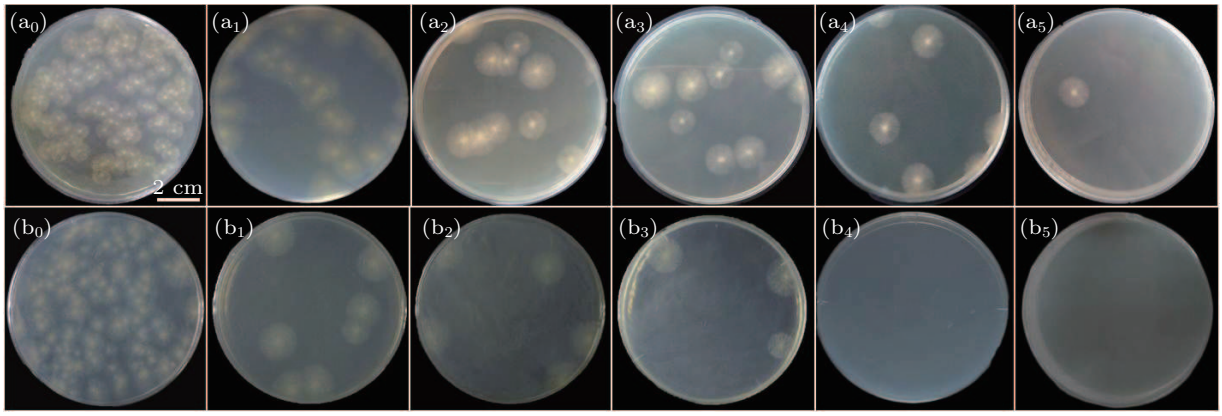


Fig. 3. (color online) The photographic illustration of the AN samples: (a_0), (b_0) the untreated silk fabric; the silk fabrics treated by the (a_1)–(a_5) Ar or the (b_1)–(b_5) Ar/O_2 APPJ plasma for 1.0 min, 2.0 min, 3.0 min, 4.0 min, and 5.0 min, respectively.

Figure 4 presents the sterilization rate of the AN attached on the silk fabrics by the Ar or Ar/O_2 plasma. The experimental data depicted by Fig. 4 showed that the sterilization rate of the silk fabrics steeped with the AN was augmented noticeably as the treatment time increased for both the Ar and the Ar/O_2 APPJ plasmas. For the Ar plasma, the sterilization rate of AN was about 77% with a treating of 1.0 min, whereas nearly 90% AN was killed by the Ar/O_2 plasma within 1.0 min with the same plasma treatment parameters. Although the exact role of the O_2 contained in the Ar/O_2 plasma for sterilization is still controversial,[35] the active species of OH and O generated in the Ar/O_2 plasma may play a crucial role for inactivating the microorganisms.[23]

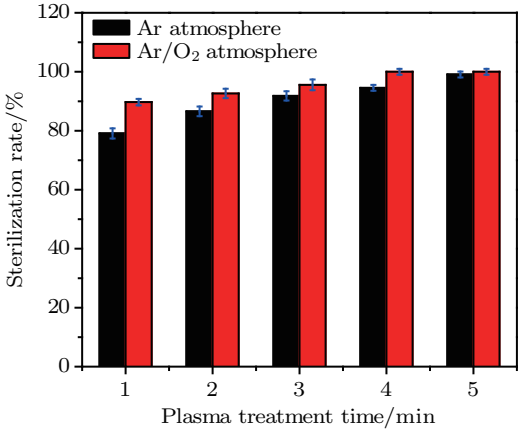


Fig. 4. (color online) The sterilization rate of the AN fungus injected onto silk fabrics treated by the Ar or the Ar/O_2 APPJ plasma with different treatment time.

It is well known that the reactive species of the APPJ system depend closely on the plasma characteristics and the discharge parameters. The AN counts on the original simulated unearthed silk fabrics (Fig. 5(a)) were about 4.2×10^5, and it decreased to 1.84×10^5 when the sample was treated by the Ar plasma with a discharge power of 30.0 W for 2.0 min (a 65.2% reduction in the AN population) (Fig. 5(c_1)). When the discharge power increased (40.0 W, 50.0 W, and 60.0 W), as shown in Figs. 5(c_2)–5(c_4), the AN counts decreased drastically (down to 2.0×10^4, a 95.2% reduction when 60.0 W was used) under the same treatment time. Such significant increase in the sterilization rate suggests that the AN can be efficiently inactivated by increasing the plasma discharge power (which understandably results in increased particle densities). In addition, the relationship between the sterilization efficiency and the discharge gas type was also investigated, and it can be seen that the Ar plasma (Fig. 5(d_2), CFU: 2.2×10^5) is more effective than the He plasma (Fig. 5(d_1), CFU: 3.8×10^5). It should be noted that the sterilization efficiencies of the He/O_2 (Fig. 5(d_3), CFU: 3.6×10^4) and the Ar/O_2 (Fig. 5(d_4), CFU: 1.8×10^4) plasmas are higher than those obtained by pure inert gases, suggesting that the presence of O_2 in the plasma jet is of essential importance.

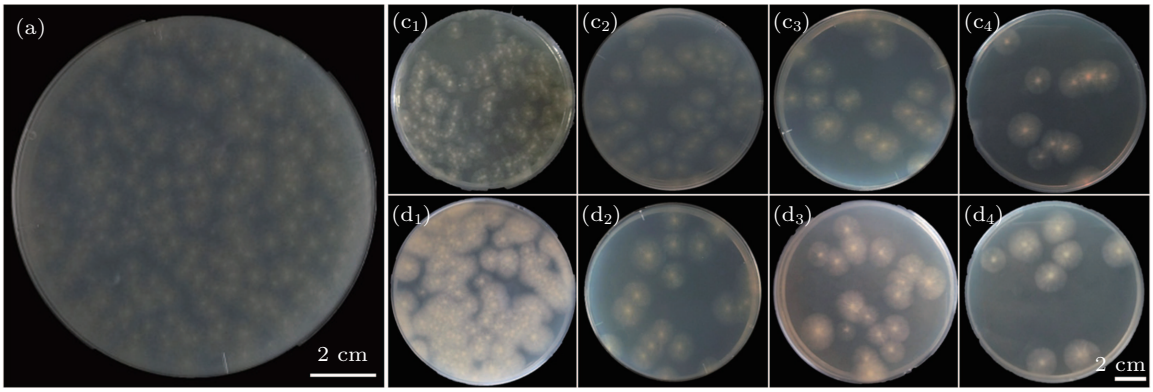


Fig. 5. (color online) The photographic illustration of the AN samples on (a) the untreated silk fabrics, and the silk fabrics treated by Ar APPJ with discharge powers of (c_1) 30.0 W, (c_2) 40.0 W, (c_3) 50.0 W, and (c_4) 60.0 W; the silk fabrics treated by (d_1) He, (d_2) Ar, (d_3) He/O_2, and (d_4) Ar/O_2 APPJ plasmas.

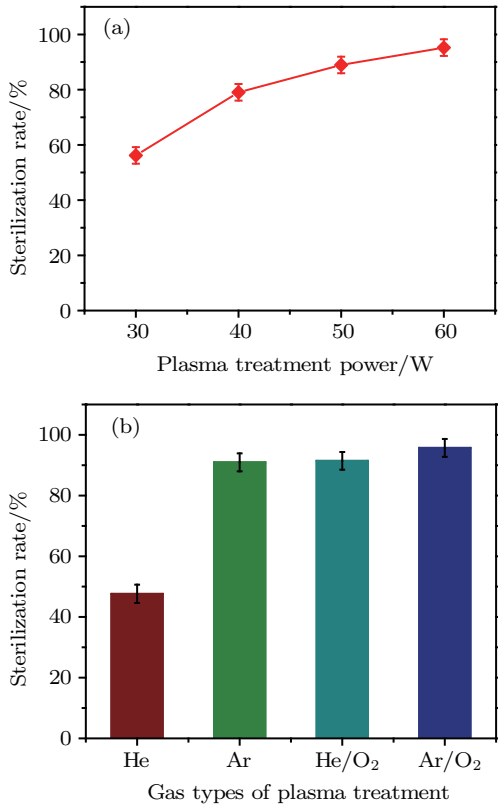


Fig. 6. (color online) The sterilization rate of the simulated unearthed silk fabrics steeped with AN treated by the APPJ plasmas with (a) different discharge powers, and (b) different gases.

In order to further explore the relationship between the sterilization rate and the discharge parameters, the effect of the discharge power and the gas types on the AN inactivation was also analyzed, as shown in Fig. 6. Figure 6(a) shows the AN reduction performance as a function of the discharge power when the Ar APPJ plasma was used. The experimental data depicted in Fig. 6(a) showed that the sterilization rate of AN increased from 56.2% (30.0 W) to 95.2% (60.0 W). Under the same discharge power of 50.0 W, the sterilization efficiency of the Ar plasma (91.0%) was nearly twice that achieved by the He plasma (47.6%). It should be particularly noted that the He/O_2 plasma could achieve almost the same sterilization performance (91.4%), suggesting once again that the presence of O_2 in the plasma jet may be crucial to the AN sterilization performance. Based on the results discussed above, the Ar/O_2 plasma is better suited for the microorganism inactivation applications than the He or He/O_2 plasma.

In order to better illustrate the morphological evolution of AN before and after plasmatic inactivation, the series digital microscope was used. Figure 7(a) shows the microscope image of the AN spores attached on the simulated unearthed silk fabrics, and the average diameter of the spore was about 86.03 μm (the inset of Fig. 7(a)). When the AN attached silk fabrics was treated by the Ar/O_2 plasma with a discharge power of 50.0 W for 4.0 min, as shown in Fig. 7(b), all the

AN spores were deformed, and the average nominal diameter of a residue of spore decreased to 34.09 μm (the inset of Fig. 7(b)). Moreover, the AN hyphas were completely destructed under the function of the Ar/O_2 plasma, resulting in permanent loss in the meristem ability. Figures 7(c) and 7(d) exhibit the three-dimensional images of the AN spores having undergone treatments by the Ar/O_2 plasma, and that the spore wall was breached by the reactive species generated in the Ar/O_2 APPJ system, as indicated by the tissue fluid that has flown out from the AN spore. From the captured images of the AN spores, the inactivation processes and mechanism of spores by the APPJ plasma may be described as follows. (i) The active species (e.g. Ar^+, O, OH, O_3, UV light) generated in the Ar/O_2 plasma firstly etch or oxidize the spore walls and hyphas.[36–38] (ii) The tissue fluids flow out from the holes on the breached spore walls while the spores are continuously oxidized by the active species.[39–41] (iii) Finally, the spores die without getting enough alimentation, and the AN lose the function of reproduction and the ability of self-replication.[38,42–45]

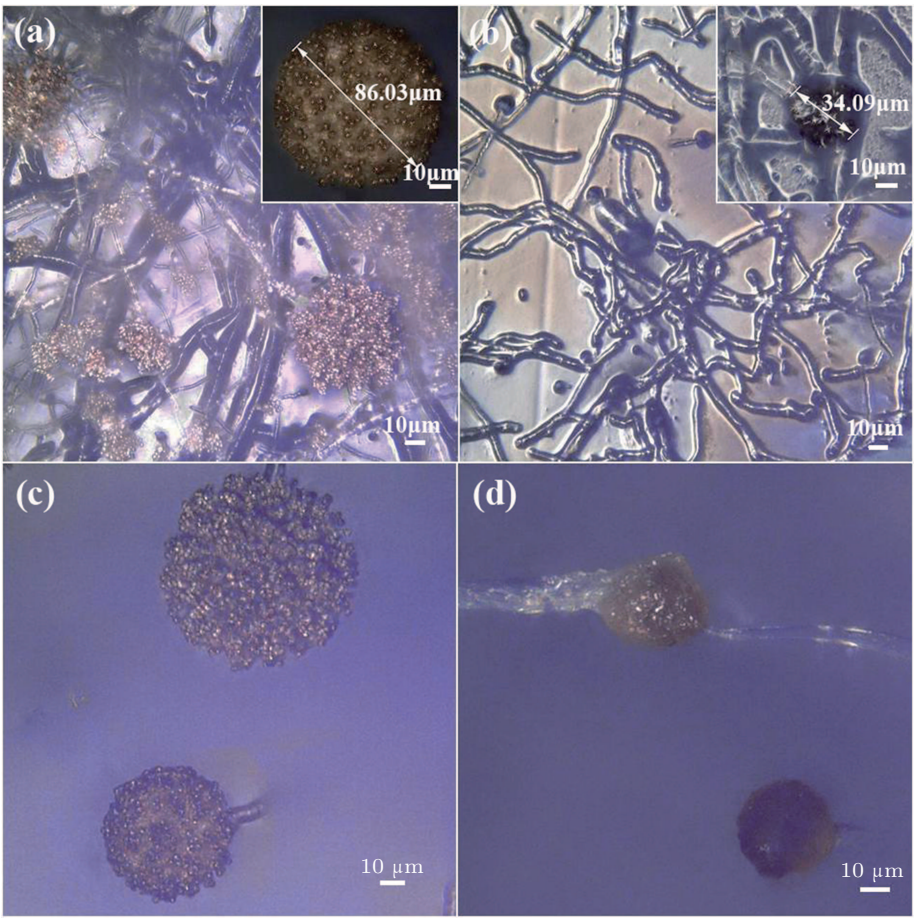


Fig. 7. (color online) The digital microscope images of AN spores: (a) and (c) untreated, (b) and (d) treated by Ar/O_2 APPJ.

Figure 8 shows the SEM images of the AN attached silk fabrics treated by the Ar/O_2 (volumetric ratio: 5/1) APPJ with different time. Compared with the untreated silk fabrics (Fig. 8(a)), there is no observable change in the surface morphology of the sample treated with the Ar/O_2 plasma for 2.0 min (Fig. 8(b)). Under the same discharge power (50.0 W), the silk fabric profiles were similarly very smooth, independent of the treatment time (3.0 min in Fig. 8(c) and 4.0 min in Fig. 8(d)). Furthermore, the effect of the plasmatic treatment time on the silk fabrics' morphology was also investigated using the high resolution SEM images (insets of Fig. 8), and the Ar/O_2 plasma left the silk fibre almost intact, as opposed to what it did to the AN fungi. Such a noticeable mitigation of the adverse destructive effects of the Ar ions showed that the Ar ions pushed by a high electric field bombard the substrate with very high velocities was attributed to the nonexistence of a strong electric field between the inner electrode and the substrate.[46] Consequently, the velocity of the Ar ions was similar to the gas flow rate, and the etching effect of the Ar ions on the silk fibre was negligible.

In order to enhance the storability of the plasmatic sterilized unearthed silk fabrics, it is of vital importance that such plasmatic treatment should have minimal impact on the physical/chemical/mechanical properties of the treated silk fabrics. Figure 9 presents the mechanical property of the silk fabrics treated by the Ar/O_2 APPJ with different time, and the elon-

gation at break and tensile strength of the samples were tested using an electronic universal testing machine controlled by a microcomputer. As the black line shows in Fig. 9, there was an upward trend for the elongation at the initial stage, and the elongation values at break changed marginally after a critical treatment time of about 40 s. Compared with the original sample, the elongation at break increased by about 10.0% when 100% sterilization of the AN on the silk fabrics was achieved by the Ar/O_2 plasma in 4.0 min. Such experimental results showed that contrary to reducing the mechanical strength of the silk fabrics, the Ar/O_2 plasma treatment performed in this work actually enhanced it. Such an increase in mechanical strength was attributed to the surface modification during the plasma treatment process. It should be noted, however, that the tensile strength did decline slightly in the initial plasma process (60 s). Beyond this point, on the other hand, the further change in the tensile strength of the plasma treated silk fabrics tended to be negligible. Such a marginal intensity decrease indicates that the physical damage of the Ar/O_2 plasma on the silk fibre can be safely neglected.

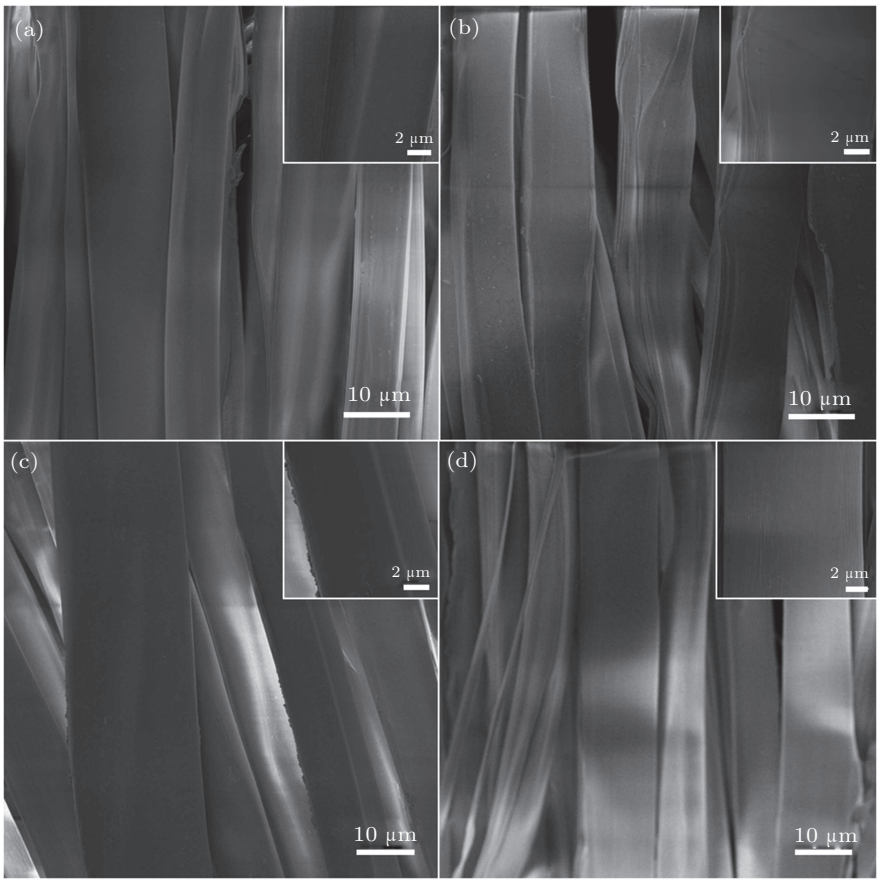


Fig. 8. The SEM micrographs of silk fabrics injected by fungus with (a) untreated; and different plasma-treated time for (b) 2.0 min, (c) 3.0 min, and (d) 4.0 min, respectively.

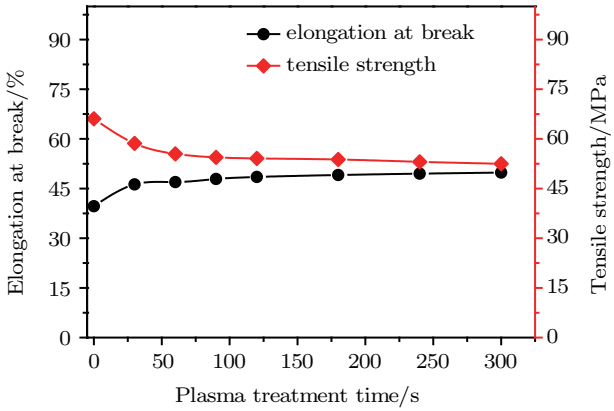


Fig. 9. (color online) The mechanical properties of the silk fabrics treated by the Ar/O_2 APPJ for different time.

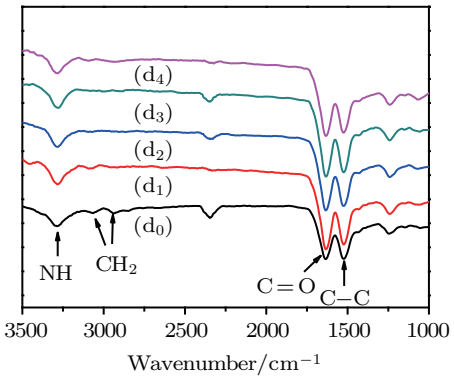


Fig. 10. (color online) FTIR absorption spectra of the silk fabrics treated by different gases with a discharge power of 50.0 W: (d_0) original sample injected with AN, (d_1) He, (d_2) Ar, (d_3) He/O_2 (Vol: 5/1), and (d_4) Ar/O_2 (Vol: 5/1).

Since the major components of both the silk fabrics and the AN are proteins and saccharides, it is important to confirm the selectivity of the active species sterilizing the silk fabrics towards the AN. The FTIR spectroscopy in ATR mode was used to investigate the compositional changes of the plasma treated silk fabrics. Figure 10 exhibits the FTIR spectra of the silk fabrics treated with different gases, and the significant peaks in line d_0 indicate that the original silk fabrics injected with the AN were covered with proteins and a small amount of sugar and chitin.[21] Compared with the original untreated silk fabric sample, no obvious change of peak positions, especially peaks of –NH at 3300 cm^{-1} and C=O at 1625 cm^{-1}, occurred in the FTIR curves for the samples treated by the He (line d_1) and the He/O_2 (line d_3) plasmas for 2.0 min. Meanwhile, similar phenomena were also observed in the samples treated by the Ar (line d_2) and the Ar/O_2 (line d_4) plasmas. It should be noted that the peak intensities of the treated samples at 1625 cm^{-1} for C=O and 1520 cm^{-1} for C–C increased noticeably. The results indicated that the active species generated by the APPJ system do not alter the chemical structure of the silk fibre, but only the DNA and cytoderm of the AN.

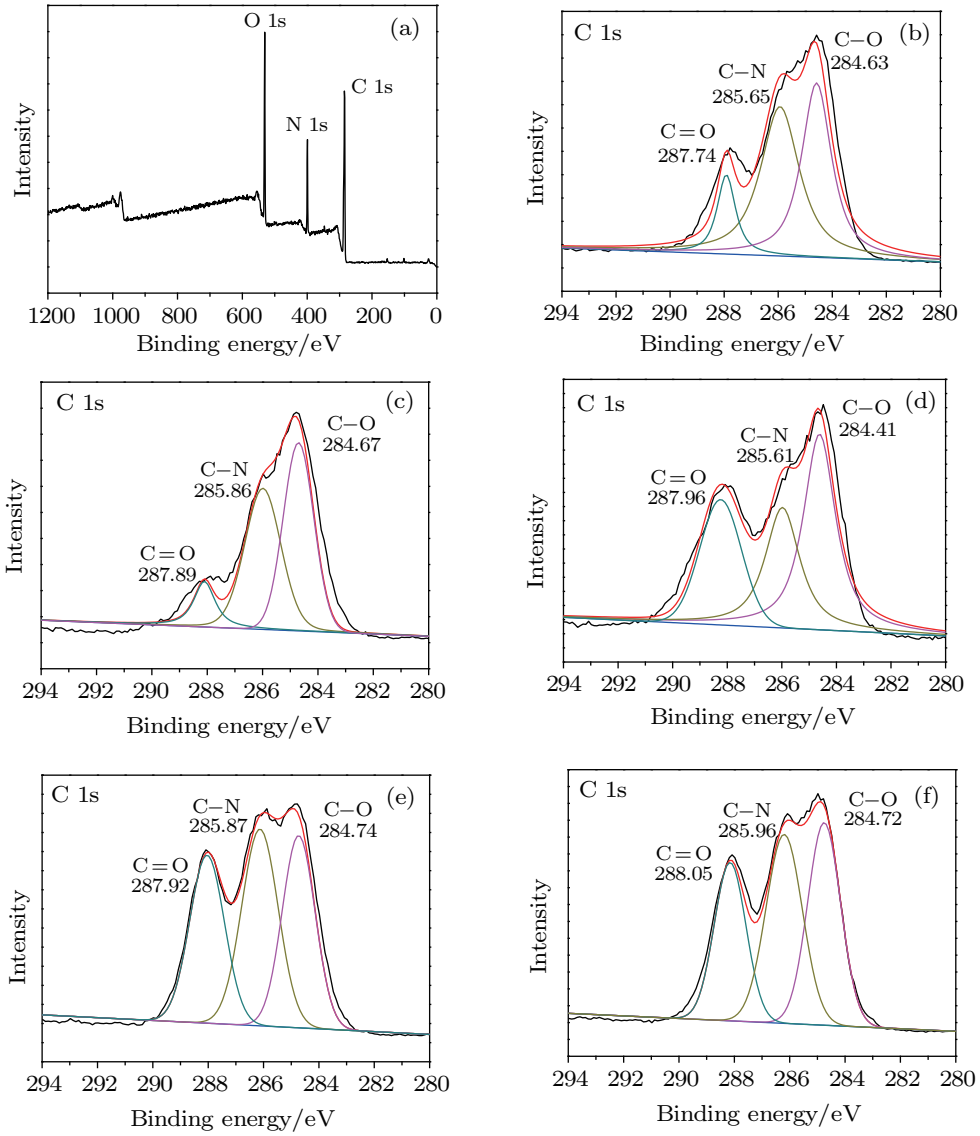


Fig. 11. (color online) (a) The XPS survey and high resolution carbon of original silk fabrics, and C 1s peaks of silk fabrics (b) untreated, and treated with different gases: (c) He, (d) Ar, (e) He/O_2, and (f) Ar/O_2.

In order to further explore the possible changes in the chemical composition of the samples before and after the plasmatic sterilization, the silk fabrics treated by the APPJ system employing different gases were characterized by an x-ray photoelectron spectrometer. Figure 11 shows the XPS survey and the high resolution C 1s of the silk fabrics surface treated by the Ar (O_2) or the He (O_2) APPJ plasma. As shown in Figs. 11(a) and 11(b), the elements on the original fabric surface injected AN were C, N, and O, and the chemical assignment for the deconvoluted carbon peaks was based on the

binding energy from the literature:[47,48] C–C/C–H (284.6 eV), C–OH/C–N (285.9 eV), C=O (287.9 eV), and C–C–OH/C–C–OR (288.7 eV). Compared with the carbon peak of the original sample (Fig. 11(b)), the chemical bonds of the silk fabrics treated by the He (Fig. 11(c)), Ar (Fig. 11(d)), He/O_2 (Fig. 11(e)), and Ar/O_2 (Fig. 11(f)) APPJ plasmas differed noticeably, especially the change of the C=O bond. The C=O bonds mainly existed in the protein of the silk fabrics and chitin of the cell wall, and a small part of them may come from the unsaturated fatty acid and protein in the mycete cells. The peak intensity of the C=O bond is relatively weak in Fig. 11(c), and the possible reason is that the mycetes covered the surface protein of the silk fabrics due to the lower sterilization efficiency of the He plasma (47.6%). Meanwhile, some of the charged particles were gathered on the surface of the cell wall, destroying the chitin structure. However, the peak intensity of the C=O bond is relatively strengthened in Figs. 11(d)–11(f), and it may be due to the destruction of the AN by the active species (e.g. Ar^+, O, OH, O_3), which is also indicated by the fact that the carbon contents of all treated samples decreased (Table 2). On the other hand, the average diameter of spores became smaller with the increased sterilization efficiency of Ar, He/O_2 and Ar/O_2 plasmas, therefore, the exposed area of the silk fabrics increased. Moreover, the oxidation species of O, OH, and O_3 destroyed the cell membrane, resulting in the outflow of protein containing C=O bonds. It should be noted that the oxygen contents of all the samples treated by the APPJ plasmas employing different gases also increased obviously, mainly attributed to the grafted O and OH radicals, which can destroy unsaturated fatty acids and exert strong oxidative effects on the outer structure of the mycete cells.[38,42]

Table 2. The surface element composition ratio of the samples treated by APPJ with different gases.

Element	C 1s	N 1s	O 1s
Control sample	65.1	14.19	20.71
He atmosphere	46.59	10	43.42
Ar atmosphere	53.75	16.14	30.11
He/O_2 atmosphere	35.88	18.61	45.52
Ar/O_2 atmosphere	35.07	16.73	48.2

4. Conclusion

In summary, a novel sterilization method employing an APPJ system is successfully implemented to sterilize mycete attached on simulated unearthed silk fabrics. The sterilization performance of AN attached on the silk fabrics depends closely on the discharge parameters of the APPJ plasma, and a longer treating time (up to 4 min) and a sufficiently higher discharge power (up to 60 W) are more beneficial when destroying the AN spores is concerned. Amongst the various plasma jets tested in this work, the Ar/O_2 APPJ plasma has been proven to be the most effective. Typically, the AN injected on silk fabrics were completely inactivated by the Ar/O_2 APPJ plasma with a treatment time of 4 min and the elongation at break strengths of the treated silk fibre increased about 10%. The experimental results showed that the Ar/O_2 APPJ plasma could successfully inactivate the AN attached on the silk fabrics without any significant damage to the integrity of the silk fibre. Therefore, the APPJ system presented in this work should be considered as a viable, minimum-destructive, and high-performance protocol for sterilizing unearthed silk fabrics. The methodology presented in this work is highly recommended for archaeological applications.

References

[1] Zheng Q, Wu X F, Zheng H L and Zhou Y 2015 *Anal. Bioanal. Chem.* **407** 3861
[2] Hermes A C, Davies R J, Greiff S, Kutzke H, Lahlil S, Wyeth P and Riekel C 2006 *Biomacromolecules* **7** 777
[3] Good I L, Kenoyer J M and Meadow R H 2009 *Archaeometry* **51** 457
[4] You Q, Liu M, Liu Y, Zheng H, Hu Z, Zhou Y and Wang B 2017 *ACS Sensors* **2** 569
[5] Li M Y, Zhao Y, Tong T, Hou X H, Fang B S, Wu S Q, Shen X Y and Tong H 2013 *Polymer Degradation and Stability* **98** 727
[6] Ball P 2009 *Nature* **457** 945
[7] Ryder M L 1996 *Textiles Magazine* **25** 15
[8] Scott B 1973 *Journal of the Royal Society of Arts* **121** 758
[9] Shahidi S and Ghoranneviss M 2013 *Plasma Science and Technology* **15** 1031
[10] Priehn M, Denis B, Aumeier P, Kirchner W, Awakowicz P and I Leichert L 2016 *J. Phys. D: Appl.Phys.* **49** 374002
[11] Javid A, Kumar M and Han J G 2017 *Appl. Surf. Sci.* **392** 1062
[12] Heinlin J, Morfill G, Landthaler M, Stolz W, Isbary G, Zimmermann J L, Shimizu T and Karrer S 2010 *J. Dtsch. Dermatol. Ges.* **8** 968
[13] Moreau M, Orange N and Feuilloley M 2008 *Biotechnolgy Advances* **26** 610
[14] Setareh S and Dorranian D 2013 *Plasma Science and Technology* **15** 1122
[15] Khamsen N, Onwimol D, Teerakawanich N, Dechanupaprittha S, Kanokbannakorn W, Hongesombut K and Srisonphan S 2016 *ACS Appl. Mater. Interfaces* **8** 19268
[16] Sakai Y, Liu Z, Goto M and Hayashi N 2016 *Jpn. J. Appl. Phys.* **55** 07L001
[17] Klämpfl T G, Isbary G, Shimizu T, Li Y F, Zimmermann J L, Stolz W, Schlegel J, Morfill G E and Schmidt H U 2012 *Applied and Environmental Microbiology* **78** 5077
[18] Laroussi M 2002 *IEEE Transactions on Plasma Science* **30** 1409
[19] Liang Y, Wu Y, Sun K, Chen Q, Shen F, Zhang J, Yao M, Zhu T and Fang J 2012 *Environmental Science & Technology* **46** 3360
[20] Keudell A, Awakowicz P, Benedikt J, Raballand V, Yanguas-Gil A, Opretzka J, Flötgen C, Reuter R, Byelykh L, Halfmann H, Stapelmann K, Denis B, Wunderlich J, Muranyi P, Rossi F, Kylián O, Hasiwa N, Ruiz A, Rauscher H, Sirghi L, Comoy E, Dehen C, Challier L and Deslys J P 2010 *Plasma Processes and Polymers* **7** 327
[21] Nobuya H, Yoshihito Y, Akira Y and Masaharu S 2014 *Jpn. J. Appl. Phys.* **53** 05FR03
[22] Sands B L, Ganguly B N and Tachibana K 2008 *Appl. Phys. Lett.* **92** 151503
[23] Zhang X, Liu D, Song Y, Sun Y and Yang S Z 2013 *Physics of Plasmas* **20** 053501
[24] Li X, Yuan N, Jia P and Chen J 2010 *Physics of Plasmas* **17** 093504
[25] Zhang X, Zhou R, Rusen Z, Chen M, Li J, Sun Y, Chen Q, Yang S Z and Huo Liu Q 2015 *Plasma Process* **13** 429
[26] Nakano Y, Fujimura S, Sato T, Kikuchi T, Ichinose M and Watanabe A 2015 *Journal of Medical and Biological Engineering* **35** 626
[27] Zheng X, Chen G, Zhang Z, Lv G, Beem J, Massey S and Tatoulian M 2013 *Plasma Processes and Polymers* **10** 379
[28] Léveillé V and Coulombe S 2005 *Plasma Sources Science and Technology* **14** 467

[29] Lee Y H, Yi C H, Chung M J and Yeom G Y 2001 *Surface and Coatings Technology* **146** 474
[30] Dong-cheol S and Tae-hun C 2001 *J. Phys. D: Appl.Phys.* **34** 2854
[31] Lu X, Xiong Q, Xiong Z, Hu J, Zhou F, Gong W, Xian Y, Zou C, Tang Z, Jiang Z and Pan Y 2009 *J. Appl. Phys.* **105** 043304
[32] Marlon H G M, Carlos V P U and Rafael Cabanzo H 2003 *Plasma Sources Science and Technology* **12** 165
[33] Massines F, Gouda G, Gherardi N, Duran M and Croquesel E 2001 *Plasmas and Polymers* **6** 35
[34] Zheng X, Chen G, Zhang Z, Beem J, Massey S and Huang J 2013 *Surface and Coatings Technology* **226** 123
[35] Schinke R and McBane G C 2010 *The Journal of Chemical Physics* **132** 044305
[36] Johnston H S 1992 *Annu. Rev. Phys. Chem.* **43** 1
[37] Matsumi Y and Kawasaki M 2003 *Chemical Reviews* **103** 4767
[38] Walsh J L and Kong M G 2008 *Appl. Phys. Lett.* **93** 111501
[39] Chang J S 2001 *Science and Technology of Advanced Materials* **2** 571
[40] Haruhiko A, Masahiro Y and Nobuo F 2008 *Jpn. J. Appl. Phys.* **47** 1435
[41] Gomez E, Rani D A, Cheeseman C R, Deegan D, Wise M and Boccaccini A R 2009 *Journal of Hazardous Materials* **161** 614
[42] Sun P, Sun Y, Wu H, Zhu W, Lopez J L, Liu W, Zhang J, Li R and Fang J 2011 *Appl. Phys. Lett.* **98** 021501
[43] Stoffels E, Sakiyama Y and Graves D B 2008 *IEEE Transactions on Plasma Science* **36** 1441
[44] Wang D, Zhao D, Feng K, Zhang X, Liu D and Yang S 2011 *Appl. Phys. Lett.* **98** 161501
[45] Laroussi M 2005 *Plasma Processes and Polymers* **2** 391
[46] Bin R, Zhang G, Ji H, Luo L, Shi P and Wang X 2017 *Journal of Nuclear Materials* **494** 55
[47] Sarani A, Nikiforov A Y, De Geyter N, Morent R and Leys C 2011 *Appl. Surf. Sci.* **257** 8737
[48] Benedikt J, Focke K, Yanguas-Gil A and Keudell A 2006 *Appl. Phys. Lett.* **89** 251504